

Lattice dynamical study of $\text{Zr}_{0.85}\text{Ca}_{0.15}\text{O}_{1.85}$ and CeO_2

This article has been downloaded from IOPscience. Please scroll down to see the full text article.

1995 J. Phys.: Condens. Matter 7 7823

(<http://iopscience.iop.org/0953-8984/7/40/013>)

View [the table of contents for this issue](#), or go to the [journal homepage](#) for more

Download details:

IP Address: 171.66.16.151

The article was downloaded on 12/05/2010 at 22:14

Please note that [terms and conditions apply](#).

Lattice dynamical study of $\text{Zr}_{0.85}\text{Ca}_{0.15}\text{O}_{1.85}$ and CeO_2

B Strauß†, H Boysen†, F Frey†, U Steigenberger‡, F Güthoff§,
A Krimmel§, H M Mayer§ and D Welz§

† Institut für Kristallographie und Mineralogie, Universität München, Theresienstrasse 41, 80333 München, Germany

‡ ISIS Facility, Rutherford Appleton Laboratory, Chilton, Didcot, Oxon OX11 0QX, UK

§ Hahn-Meitner-Institut, BENS, Glienickestrasse 100, 14109 Berlin, Germany

Received 24 April 1995, in final form 3 July 1995

Abstract. Inelastic neutron scattering studies of $\text{Zr}_{0.85}\text{Ca}_{0.15}\text{O}_{1.85}$ at 300, 1200 and 1500 K show LA and TA phonons rapidly broadening with phonon wavevector q in all observed directions ($[00\xi]$, $[\xi\xi 0]$, $[\xi\xi\xi]$, $[-\xi/2, -\xi/2, \xi]$). Optical phonon branches could not be observed. Both results can be related to the underlying static disorder. Comparative studies of well ordered CeO_2 show that the influence of anharmonicities is negligible in both these oxides up to temperatures of 1500 K. The phonon linewidths of $\text{Zr}_{0.85}\text{Ca}_{0.15}\text{O}_{1.85}$ are exceptionally large at 1200 K. This can be related to phase diagram boundaries occurring in this temperature regime. The temperature dependence of the linewidths is associated with the hindered cubic:tetragonal phase transition. The line broadening is markedly anisotropic. Elastic constants c_{11} , c_{12} and c_{44} were derived from the data at 1200 K.

1. Introduction

Pure ZrO_2 exists at ambient pressure in three polymorphs: cubic ($Fm\bar{3}m$) above 2640 K, tetragonal ($P4_2/nmc$) between 2640 K and 1420 K and monoclinic ($P2_1/c$) below 1420 K. By adding appropriate oxides such as CaO or Y_2O_3 the high-temperature structure(s) can be stabilized at room temperature. Due to the aliovalent cations, oxygen vacancies are created which are partially correlated. The defect structure of zirconia doped with 15 mol% CaO has been investigated by Neder *et al* (1990), Rossell *et al* (1991), Wellberry *et al* (1993) and Proffen *et al* (1993). Characteristic diffuse scattering with diffuse maxima at positions $\pm(0.4, 0.4, \pm 0.8)$ is observed in this material. According to Neder *et al* (1990) it can be described by a distribution of correlated microdomains. A first type of microdomain is based on a single oxygen vacancy with relaxed neighbouring ions. A second type is based on two oxygen vacancies separated by $1/2\sqrt{3}$ along $\langle 111 \rangle$. There is still some controversy in the literature about this model. For our purpose it is sufficient to accept that the oxygen vacancies are not distributed randomly. Around 1300 K the intensities of the diffuse maxima decrease markedly (Proffen *et al* 1993). The half-widths and shapes of the diffuse intensity distributions stay nearly unchanged. This process was observed to be reversible in several cycles of heating and cooling the sample. It may be concluded, therefore, that the amount of correlated microdomains decreases with increasing temperature, whereas the correlation remains unaffected. Roughly in the same temperature regime the phase diagram (Hellmann and Stubican 1983) exhibits boundaries between the $M_{ss} + \Phi_1$, $T_{ss} + \Phi_1$ and C_{ss} coexistence fields to be close together (M_{ss} is a monoclinic solid solution, T_{ss} is a tetragonal solid solution, C_{ss} is a cubic solid solution and Φ is an ordered intermediate phase). A dynamic origin for the phase transition mechanism has been proposed in the literature. Negita (1989)

suggests that the instability of the phonon modes at the cubic Brillouin zone boundary X point, $(0, 0, 2\pi/a)$, is associated with the successive cubic-to-tetragonal and tetragonal-to-monoclinic phase transition in pure ZrO_2 . Keramidis and White (1973) studied the lattice dynamics of a series of solid solutions in the CaO-ZrO_2 system by Raman spectroscopy. Liu *et al* (1987) investigated the lattice dynamics of the closely related yttria-stabilized zirconia with 20 wt% of Y_2O_3 by inelastic neutron scattering. The aim of the present study was to investigate the temperature dependence of the lattice dynamics of $\text{Zr}_{0.85}\text{Ca}_{0.15}\text{O}_{1.85}$ with respect to the phase boundaries and the changes in disorder mentioned above. Pure ceria (CeO_2) has the ideal, well ordered fluorite structure. It was therefore used as a 'reference' in this investigation. The lattice dynamics of CeO_2 at 293 K have been previously investigated by Clausen *et al* (1987).

2. Experimental details

The single crystals of $\text{Zr}_{0.85}\text{Ca}_{0.15}\text{O}_{1.85}$ used in this study, grown by the skull melting method, were provided by Djvahirdjan SA, Monthey, Switzerland. The sample size was about $10\text{ mm} \times 10\text{ mm} \times 15\text{ mm}$. The measurements on $\text{Zr}_{0.85}\text{Ca}_{0.15}\text{O}_{1.85}$ were carried out on the time-of-flight spectrometer PRISMA at the neutron spallation source ISIS at Oxford, UK (Steigenberger *et al* 1991) and the triple-axis spectrometer E7 at the Berlin Neutron Scattering Center at Berlin, Germany.

In the case of the measurements at PRISMA a RAL furnace with a niobium heating element was used. The sample was sealed in a niobium can to prevent loss of oxygen when heated in vacuum. The crystal was aligned to allow measurements in the $[1\bar{1}0]$ zone. Measurements of the phonon dispersion of longitudinal acoustic (LA) and transverse acoustic (TA) phonons propagating along the main symmetry directions were performed at 290, 1200 and 1500 K. Only the data measured at 1200 K could be evaluated. At 290 K the phonon signals were too weak due to the low occupation of states. At 1500 K the sealing of the sample could not be maintained and the sample underwent an irreversible change due to reduction. After the experiment the sample was brittle and the colour had changed from transparent to black.

Therefore the measurements at the triple-axis spectrometer E7 on another sample were performed with a mirror furnace (Lorenz *et al* 1993) which operates under a normal, i.e. oxidizing, atmosphere and yields temperatures up to about 2000 K. The sample was again aligned to perform measurements in the $[1\bar{1}0]$ zone. Data were taken using the fixed k_i mode at $k_i = 2.64\text{ \AA}^{-1}$ and collimations 60–40–40–60. Pyrolytic graphite was used as a monochromator and analyser, and a pyrolytic graphite filter was placed between monochromator and sample to eliminate higher-order contamination. Scans at a constant scattering vector or at constant energy were made.

The single crystals of CeO_2 were grown by the skull method and provided by W Asmuß, University of Frankfurt, Germany. The experiments were also performed at the TAS E7 with a single crystal of dimensions $15\text{ mm} \times 17\text{ mm} \times 20\text{ mm}$. The experimental conditions were chosen to be identical with the experiments on $\text{Zr}_{0.85}\text{Ca}_{0.15}\text{O}_{1.85}$ to achieve comparable data.

3. Results and discussion

The results of the ISIS experiment at 1200 K are shown in figure 1. This overview shows TA and LA dispersion branches along the main symmetry directions. A considerable

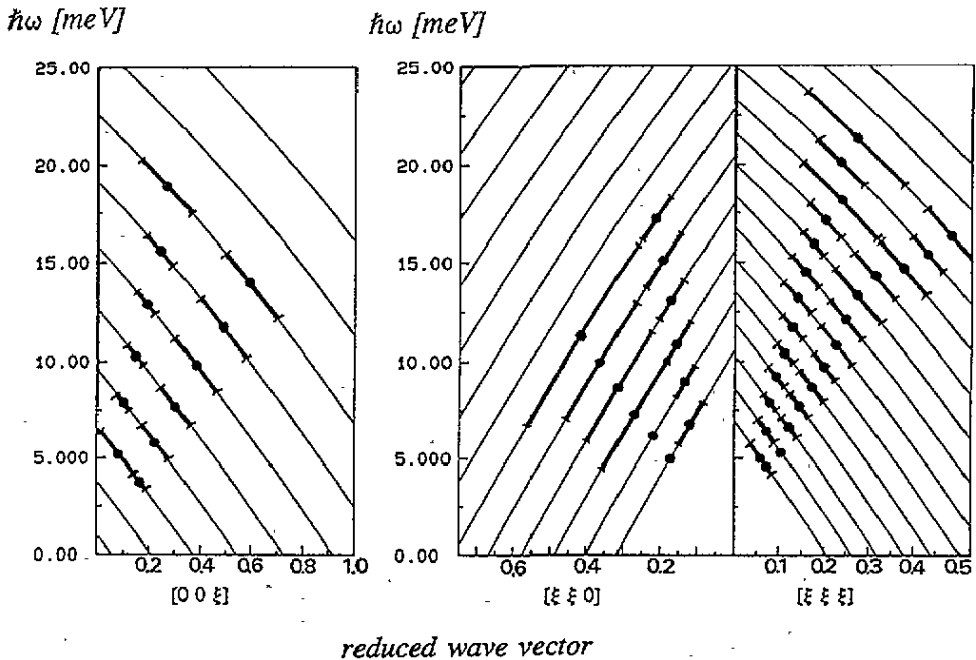
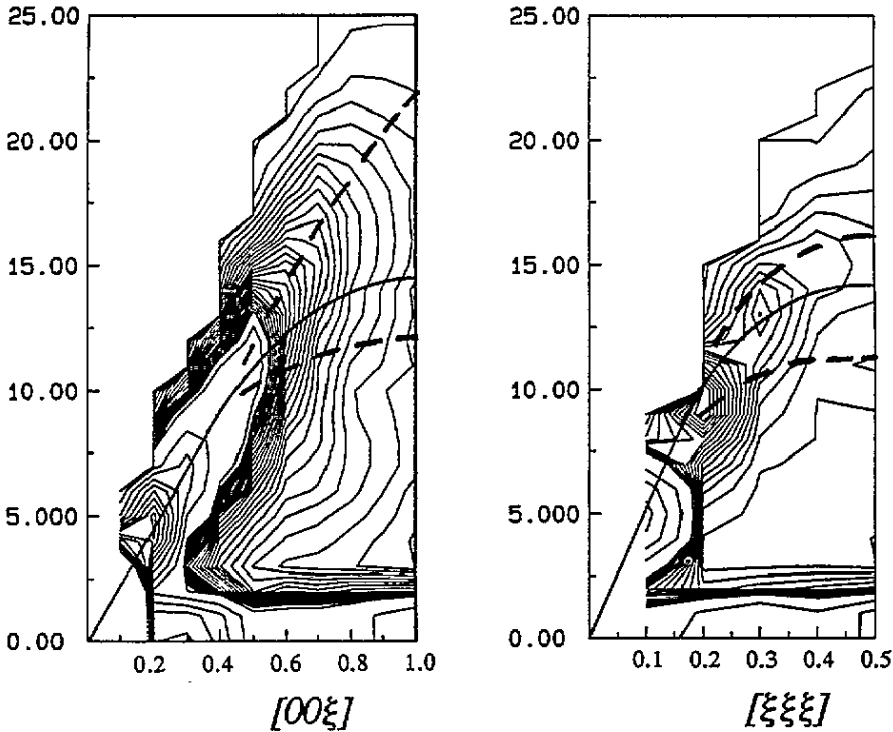


Figure 1. All dispersion curves measured on $Zr_{0.85}Ca_{0.15}O_{1.85}$ at 1200 K at the time-of-flight spectrometer PRISMA; the full circles represent the positions and the highlighted lines the linewidths of the Gaussians fitted to the data. No optical phonon modes were observed.

broadening of all acoustic modes was observed with increasing phonon wavevector q ($[00\xi]$, $[\xi\xi 0]$, $[\xi\xi\xi]$) which is much larger than the resolution of the spectrometer. Due to the geometry of the PRISMA spectrometer (Steigenberger *et al* 1991), the data are taken along parabolae-shaped trajectories in the (Q, E) -space. The raw data collected in each of the 16 detectors of PRISMA were fitted by Gaussian functions to determine positions and half-widths of each peak. Phonons propagating along the $[111]$ direction could be observed up to the Brillouin zone boundary: along the $[100]$ and $[110]$ directions the signals broaden more rapidly and become unobservable at the zone boundaries. No signals of any optical phonons could be detected.

The results were complemented by further experiments at the triple-axis spectrometer E7. Constant- Q scans representative for the TA branches in the directions $[00\xi]$ and $[\xi\xi\xi]$ are displayed in figure 2 as contour maps in the (Q, E) -space. This type of representation demonstrates impressively the broadening of the signals. The lineshapes of the phonons as a function of the reduced phonon wavevector component ξ and energy $\hbar\omega$ were assumed to be Lorentzian in form. The neutron groups were therefore fitted by a convolution of a Lorentzian with a normalized Gaussian with widths calculated for the resolution of the spectrometer at the position of the maximum. The results of these 'single-line fits' are shown in figure 3. At energy transfers well above about 8 meV all observed peaks due to TA modes show an asymmetric line shape and a trend to split into two peaks. Therefore more accurate fits could be obtained using two peaks to describe these spectra. The positions of these 'two-line fits' are also shown in figure 3. Figure 4 shows examples of the application of both methods of fitting the data measured at the reciprocal position $(1.3\ 1.3\ 2.7)$. Again no optical phonons were observable. All acoustic phonons observed on $Zr_{0.85}Ca_{0.15}O_{1.85}$

$\hbar\omega$ [meV] $\hbar\omega$ [meV]

reduced wave vector

Figure 2. Contour map of constant- Q scans representative of the TA branches in directions $[00\xi]$ and $[\xi\xi\xi]$ at $T = 1200$ K. The full and broken curves mark the positions of the Lorentzians determined by 'single-line fits' and 'two-line fits', respectively. The measurement was performed at the triple-axis spectrometer E7.

broaden rapidly. The transverse modes show a behaviour characteristic of resonance modes, with shoulders on the peaks with increasing wavevector and a pronounced splitting of the signal near the zone boundary due to the local breaking of symmetry. The widths of the longitudinal phonons are in general smaller than those of the transverse phonons and show no indication of the existence of a resonant perturbation. There is a noticeable anisotropy between the main symmetry directions. The linewidths of the phonons propagating along $[111]$ are generally smaller than those propagating along $[110]$ or $[100]$. Note also that $TA_{[110]}[00\xi]$ and $TA_{[001]}[\xi\xi 0]$ are related to the elastic constant c_{44} while $TA_{[112]}[\xi\xi\xi]$ corresponds to $(c_{11} - c_{12} + c_{44})/3$. From the slope of the long-wavelength part of the measured dispersion relations the elastic constants of $Zr_{0.85}Ca_{0.15}O_{1.85}$ are calculated as $c_{11} = 3.20 \pm 0.03$ N m $^{-2}$, $c_{12} = 1.46 \pm 0.04$ N m $^{-2}$ and $c_{44} = 0.51 \pm 0.03$ N m $^{-2}$ at 1200 K.

A further point of interest is the behaviour of the modes in the direction towards a diffuse maximum (see introduction), i.e. a $[\bar{1}\bar{1}2]$ direction. The dispersion was measured at 1200 K as shown in figure 5. The slope of the long-wavelength part of the dispersion corresponds to the slope calculated from the elastic constants determined along symmetry directions.

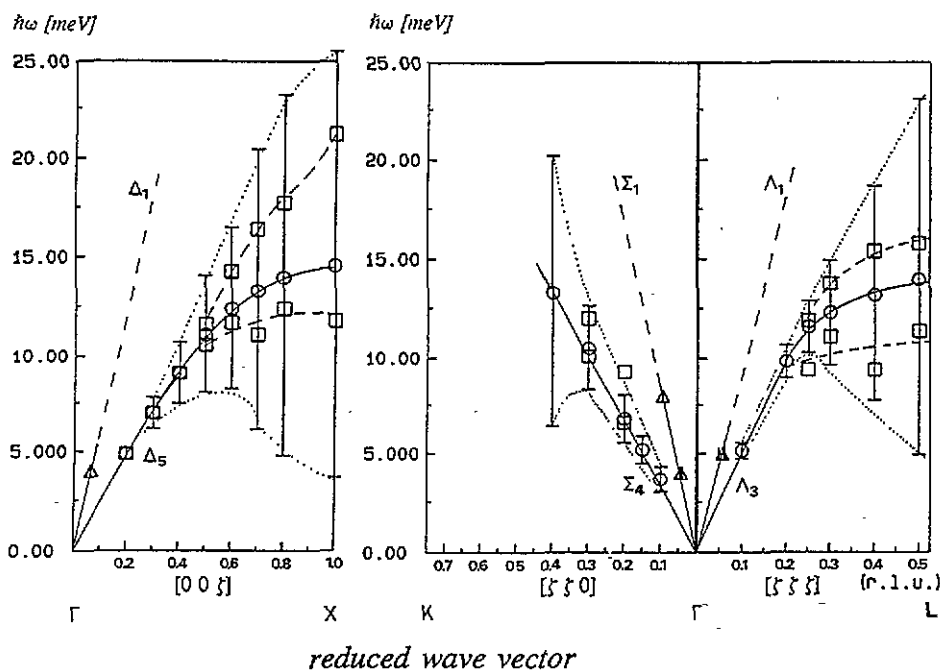


Figure 3. All dispersion curves measured on $Zr_{0.85}Ca_{0.15}O_{1.85}$ at $T = 1200$ K at the triple-axis spectrometer E7; the bars represent linewidths of the Lorentzians with (and not the errors in position) determined from the data shown in figure 2 by 'single-line fits'. The squares mark the positions of the 'two-line fits'. No optical phonon modes were observed.

Thus the average cubic symmetry is preserved, i.e. there is no special anomaly which might have been expected, if the diffuse peaks were interpreted as 'satellites' indicative of a static modulation wave.

The linewidths along $[\bar{1}\bar{1}2]$ broaden comparably to those in the $[100]$ direction. One may define a certain critical wavelength beyond which the perturbation of the phonon signals becomes significant for the different directions:

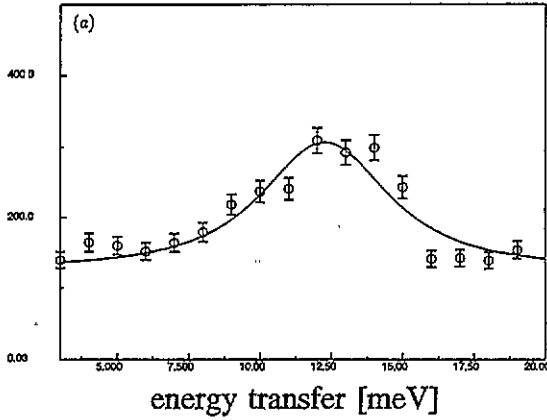
$TA_{[110]}[00\xi]$	$\xi_c = 0.40 \pm 0.03$	$\lambda_c = 13 \pm 1\text{\AA}$
$TA_{[001]}[\xi\xi 0]$	$\xi_c = 0.15 \pm 0.03$	$\lambda_c = 25 \pm 4\text{\AA}$
$TA_{[\bar{1}\bar{1}\bar{2}]}[\xi\xi\xi]$	$\xi_c = 0.20 \pm 0.03$	$\lambda_c = 15 \pm 2\text{\AA}$
$TA_{[110]}[-\xi/2, -\xi/2, \xi]$	$\xi_c = 0.20 \pm 0.03$	$\lambda_c = 21 \pm 2\text{\AA}$

where the subscript to TA denotes the polarization vector.

The phonons propagating along $[111]$ and $[001]$ directions remain undisturbed above a wavelength of about 14\AA while phonons propagating along $[110]$ and $[\bar{1}\bar{1}\bar{2}]$ directions are perturbed below about 23\AA . This dependence of the perturbation on the propagation direction of the phonon can be related to the distances between possible nearest neighbour defects. This indicates a disorder model where nearest-neighbour vacancies as well as multiple vacancies on 'empty (i.e. without cation) cubes' in the oxygen substructure are forbidden. Such an avoidance principle could explain the diffuse maxima but has to be proven by model calculations.

Figure 6 shows the dependence of the linewidths of the 'single-line fits' on wavevector and temperature. Measurements were carried out at the triple-axis spectrometer E7 at

intensity [a.u.]



intensity [a.u.]

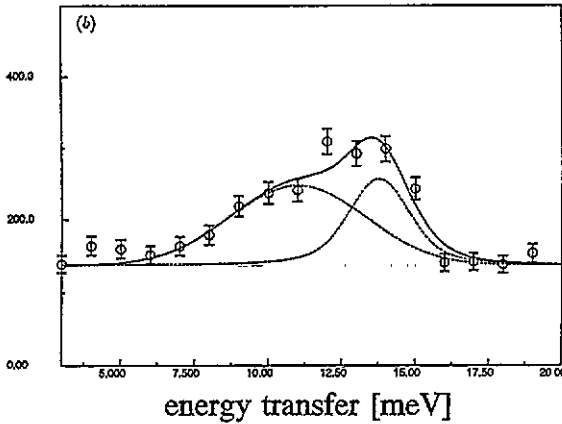


Figure 4. Examples of the application of both methods of data fitting at the reciprocal position (1.3 1.3 2.7) at $T = 1200$ K (a.u., arbitrary units): (a) single-line fit; (b) two-line fit.

temperatures of 300, 1200 and 1500 K. The linewidths at 300 and 1500 K are almost equal, while the widths at 1200 K are larger near the Brillouin zone boundary. This temperature roughly corresponds to the observed change in disorder and is close to the phase boundary. This is perhaps an indication of the expected anomaly at the cubic-to-tetragonal phase transition. A possible interpretation is that the coupling of the dynamics of the defects to the 'ordered modes' prevents the expected softening of the mode. It could be seen, however, in the linewidths as resonance-like behaviour, where all zone-boundary modes are concerned. On the other hand, it is probably exactly this suppression of well behaved phonons by disorder which prevents the phase transition from taking place via a soft-mode mechanism so that the disordered cubic phase can be retained at room temperature.

It may be noted that at small q -values the increase in the widths is roughly proportional to q^2 and independent of temperature. This is consistent with the behaviour expected for the attenuation of sound waves in the hydrodynamic or collision-dominated limit (Woodruff and Ehrenreich 1961, Kwok 1967). A similar behaviour was discussed by Liu *et al* (1987) for yttria-stabilized zirconia.

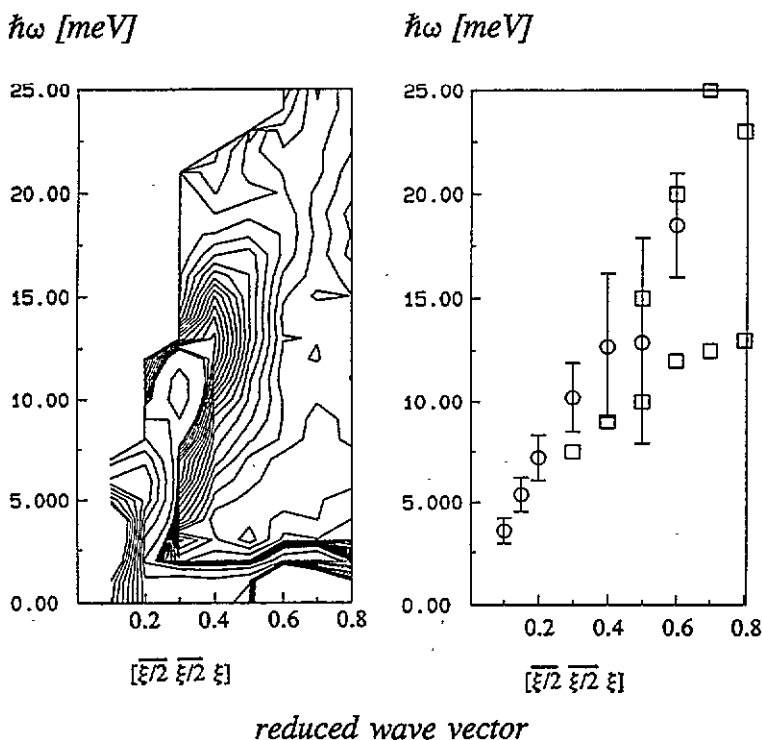


Figure 5. Contour map of constant- Q scans and dispersion curves measured on $Zr_{0.85}Ca_{0.15}O_{1.85}$ at $T = 1200$ K in the direction $[112]$ (towards the diffuse maximum). The circles and bars represent the positions and linewidths of Lorentzians determined by 'single-line fits', and the squares the results of 'two-line fits'.

The widths of all phonons in ceria are within the error limits equal to those calculated from the resolution of the spectrometer. They show no significant temperature broadening. The slight decrease in the frequencies (figure 7) with increasing temperature is comparable to those observed in $Zr_{0.85}Ca_{0.15}O_{1.85}$. We conclude that the increased linewidths measured on $Zr_{0.85}Ca_{0.15}O_{1.85}$ are completely due to disorder and the influence of temperature induced anharmonicities is negligible up to 1500 K in both these oxides. It should be noticed that intensity $\propto 1/\omega^2$ is fulfilled in CeO_2 , but not in $Zr_{0.85}Ca_{0.15}O_{1.85}$.

As mentioned before, the linewidths of phonon groups in yttria-stabilized zirconia (with 20 wt% Y_2O_3) published by Liu *et al* (1987) show a similar behaviour. Again the resonance-like behaviour is visible. Although the temperatures and the amounts of dopant cations are not exactly the same, it should be noted that the linewidths of yttria-stabilized zirconia are generally smaller than those of calcia-stabilized zirconia. This can be related to the different masses and charges of the dopant cations. The masses of Y (88.91 au) and Zr (91.22 au) are almost equal, while Ca (40.08 au) has roughly half the weight. Thus the sublattice of the metal cations is considerably more disordered in case of the calcia-stabilized zirconia.

The Raman scattering measurements of Keramidas and White (1973) for the single-phase fluorite structure with 15 mol% CaO show a complete breakdown of translational symmetry due to disorder. Thus the Raman spectra essentially represent the frequency distribution of the density of states. This result is in agreement with the fact that optical phonons cannot be observed in this investigation. The high amount of defects on the oxygen sublattice

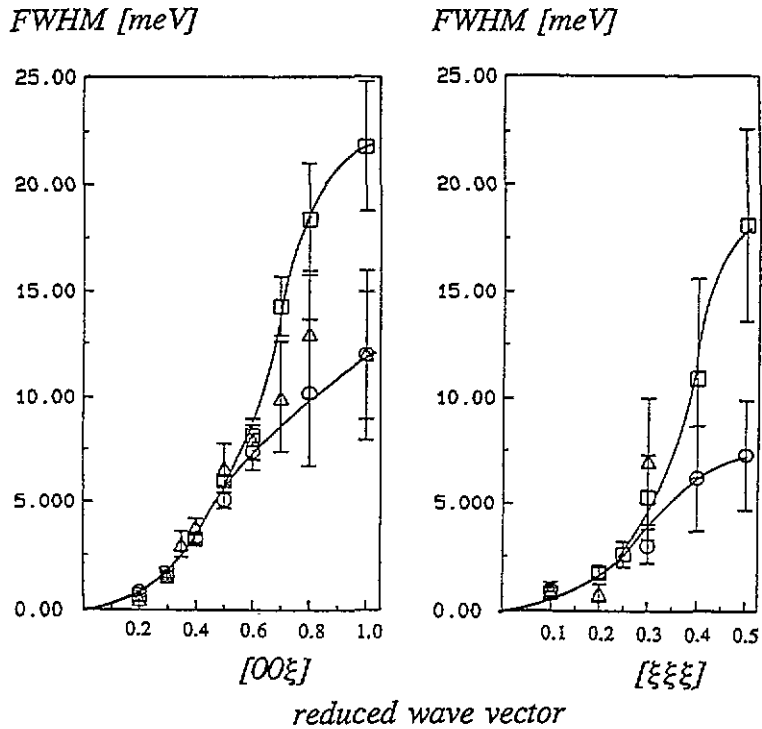


Figure 6. Wavevector and temperature dependences of the linewidths of the 'single-line fits' for $TA_{[110][00\xi]}$ and $TA_{[11\bar{2}][\xi\xi\xi]}$ of $Zr_{0.85}Ca_{0.15}O_{1.85}$: \circ , 300 K; \square , 1200 K; \triangle , 1500 K.

and the subsequent breakdown of wavevector selections does not allow well defined optical phonon branches in inelastic neutron scattering, confirming the results of Liu *et al* (1987) of inelastic neutron scattering studies of yttria-stabilized zirconia.

4. Conclusions

The frequencies and linewidths of the TA and LA phonons propagating along the principal symmetry directions in $Zr_{0.85}Ca_{0.15}O_{1.85}$ have been measured as functions of temperature up to 1500 K. No optical phonons could be observed. In agreement with this observation the Raman spectra (Keramidas and White 1973) represent the frequency distribution of the density of states.

The increased linewidths of phonon groups in $Zr_{0.85}Ca_{0.15}O_{1.85}$ are due to the underlying disorder. The comparison of the temperature dependence of linewidths in $Zr_{0.85}Ca_{0.15}O_{1.85}$ and CeO_2 shows that the influence of anharmonicities is negligible up to temperatures of 1500 K in both these oxides.

The linewidths in yttria- and calcia-stabilized zirconia indicate qualitatively a behaviour which is known as 'resonant mode behaviour' in disordered materials. Present theoretical models on the dynamics of correlated (both displacive and substitutional), disordered systems do not seem to be adequate to allow any conclusive decision as to whether vacancies, mass difference or correlations between the defects play the decisive role. The anisotropy of the broadening can be related to the specific disorder model.

The expected softening of the phonon modes at the Brillouin zone boundary X point

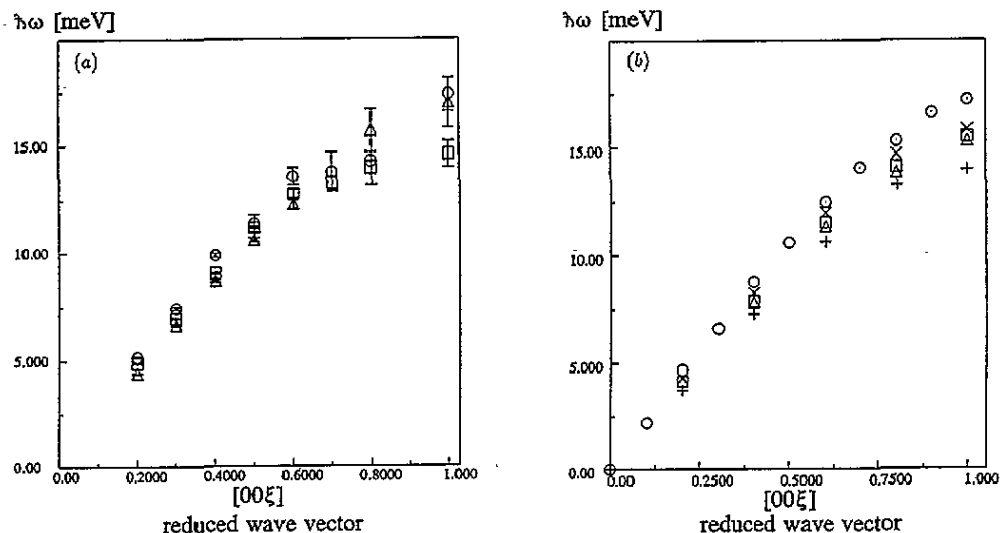


Figure 7. Temperature dependence of frequencies of $TA_{110}[00\xi]$ for (a) $Zr_{0.85}Ca_{0.15}O_{1.85}$ (O, 300 K; □, 1200 K; Δ, 1500 K) and (b) CeO_2 (O, 293 K (from Clausen *et al* 1987); X, 600 K; □, 900 K; Δ, 1050 K; (+), 1300 K).

associated with the cubic \leftrightarrow tetragonal phase transition (Negita 1989) could not be observed. The linewidths increase markedly at 1200 K. This may be related to the suppression of the phase transition. Probably it is the suppression of well behaved phonons by disorder which inhibits the phase transition from taking place via a soft-mode mechanism so that the cubic phase can be retained at room temperature.

Acknowledgment

This work was supported by funds of the BMFT under 03-SC3LMU.

References

- Clausen K, Hayes W, Macdonald E J, Osborn R, Schnabel P G, Hutchings M T and Magerl A 1987 *J. Chem. Soc., Faraday Trans. II* **83** 1109
- Hellmann J R and Stubican V S 1983 *J. Am. Ceram. Soc.* **66** 260
- Keramidas V G and White W B 1973 *J. Phys. Chem. Solids* **34** 1873
- Kwok Ph C K 1967 *Solid State Phys.* **20** 213
- Liu D W, Perry C H, Feinberg A A and Currat R 1987 *Phys. Rev. B* **36** 9212
- Lorenz G, Neder R B, Marxreiter J, Frey F and Schneider J 1993 *J. Appl. Crystallogr.* **26** 632
- Neder R B, Frey F and Schulz H 1990 *Acta Crystallogr. A* **46** 792
- Negita K 1989 *Acta Metall.* **37** 313
- Proffen TH, Neder R B, Frey F, Keen D A and Zeyen C M E 1993 *Acta Crystallogr. B* **49** 605
- Rossell H J, Sellar J R and Wilson I J 1991 *Acta Crystallogr. B* **47** 862
- Steigenberger U, Hagen M, Caciuffo R, Petrillo C, Ciffo F and Sacchetti F 1991 *Nucl. Instrum. Methods B* **53** 87
- Wellberry T R, Butler B D, Thompson J G and Whithers R L 1993 *J. Sol. Stat. Chem.* **106** 461
- Woodruff T D and Ehrenreich H 1961 *Phys. Rev.* **123** 1553